Journal of Low Temperature Physics (2020) 199:1107–1117
https://doi.org/10.1007/s10909-019-02329-w

Updated Design of the CMB Polarization Experiment Satellite LiteBIRD

H. Sugai, et al. ***[full author details at the end of the article]***

Received: 30 August 2019 / Accepted: 26 December 2019 / Published online: 27 January 2020
© The Author(s) 2020

Abstract
Recent developments of transition-edge sensors (TESs), based on extensive experience in ground-based experiments, have been making the sensor techniques mature enough for their application on future satellite cosmic microwave background (CMB) polarization experiments. LiteBIRD is in the most advanced phase among such future satellites, targeting its launch in Japanese Fiscal Year 2027 (2027FY) with JAXA's H3 rocket. It will accommodate more than 4000 TESs in focal planes of reflective low-frequency and refractive medium-and-high-frequency telescopes in order to detect a signature imprinted on the CMB by the primordial gravitational waves predicted in cosmic inflation. The total wide frequency coverage between 34 and 448 GHz enables us to extract such weak spiral polarization patterns through the precise subtraction of our Galaxy's foreground emission by using spectral differences among CMB and foreground signals. Telescopes are cooled down to 5 K for suppressing thermal noise and contain polarization modulators with transmissive half-wave plates at individual apertures for separating sky polarization signals from artificial polarization and for mitigating from instrumental $1/f$ noise. Passive cooling by using V-grooves supports active cooling with mechanical coolers as well as adiabatic demagnetization refrigerators. Sky observations from the second Sun–Earth Lagrangian point, L2, are planned for 3 years. An international collaboration between Japan, the USA, Canada, and Europe is sharing various roles. In May 2019, the Institute of Space and Astronautical Science, JAXA, selected LiteBIRD as the strategic large mission No. 2.

Keywords Satellite · Cosmic microwave background · Polarization · Inflation · Primordial gravitational wave

1 Concept of LiteBIRD

It has been suggested since the 1980s [1–3] that inflation occurred in the very early, high energy Universe, to resolve remaining issues of the Big Bang theory, such as uniformity, flatness, and monopole problems. Cosmic inflation predicts primordial gravitational wave production, with quantum fluctuations of spacetime

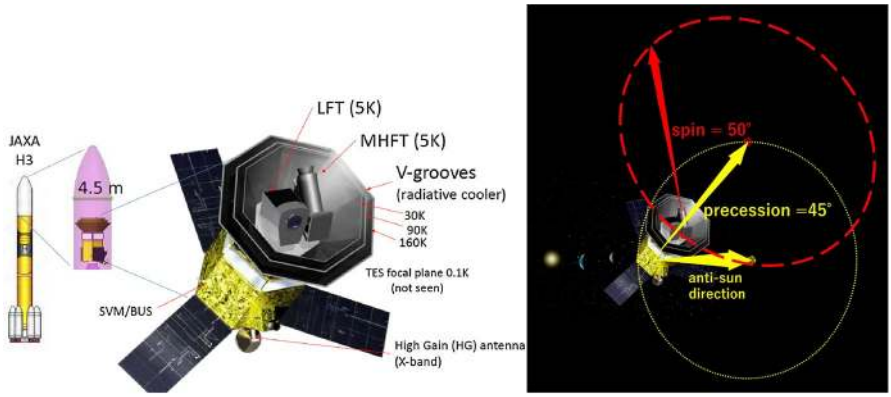

Fig. 1 *Left:* Conceptual design of LiteBIRD. Warm launch is planned with JAXA's H3 rocket. *Right:* Scans with spin angle 50° and precession angle 45° at L2. (Color figure online)

as its origin. The LiteBIRD (Lite (Light) satellite for the studies of B-mode polarization and Inflation from cosmic background Radiation Detection) aims to detect signatures of these primordial gravitational waves in the form of specific curl patterns [4, 5] of polarization angle distribution of the Cosmic Microwave Background (CMB). The sizes of expected spiral patterns in the sky are characterized by Hubble lengths at the electron scattering eras of the CMB, since primordial gravitational waves that enter the horizon in these eras most effectively produce tensor anisotropies. It is therefore essential to cover the whole sky to investigate these large Hubble lengths at the recombination era as well as the reionization era.

LiteBIRD is focused on this point: targeting [6] both the recombination era with the multipole moment l between 11 and 200 and the reionization era with l between 2 and 10, optimizing the angular resolution. The other important concepts of this satellite are a warm launch without the requirements of heavy vessels/tanks and use of multichroic detectors for the effective exploitation of finite focal-plane areas. Advantages of measurements from space are being free from atmospheric effects, providing high sensitivity, stability with less systematic uncertainties [e.g., 7], and no restrictions on observing band selection. Space measurements also give no pickup from the ground. The Sun–Earth L2 point has been selected, since the Sun, the Earth, and the Moon are all located in almost the same direction, which makes it easier to avoid facing them in terms of optical and thermal aspects. Care should be taken, however, on cosmic ray effects [8] because the satellite is more directly exposed to them. Sky observations are planned for 3 years: The presently guaranteed cooling-chain lifetime is 3.5 years, in which 0.5 year is assigned to the transitional period to the normal observation phase on course to L2. A scanning strategy with a combination of boresight spin angle of 50° around the satellite axis and its precession-like rotation around the anti-Sun direction of 45° is used (Fig. 1), since this combination provides not only a fairly

uniform sky coverage but also the minimization of instrumental systematic uncertainties in polarization measurements.

2 Status of LiteBIRD

In May 2019, the Institute of Space and Astronautical Science (ISAS), JAXA, confirmed that LiteBIRD completed activities planned during Pre-phase A2 (previously called Phase-A1 and dedicated to the concept study and development of key technologies) and selected LiteBIRD as the strategic large mission No. 2, with modifications to the cooling chain and subsequently the focal-plane designs: We have chosen to use adiabatic demagnetization refrigerators (ADRs) in series, removing ideas [6, 9] of using a JAXA-provided 1-K J-T cooler and of having 2-K telescope apertures. To recover the degraded sensitivity with 5-K apertures

Table 1 Updated basic parameters and current baseline design for LiteBIRD

Mission category	JAXA's strategic large mission
Launch vehicle	H3-22L or equivalent
Launch schedule	2027FY
Ground station	JAXA's ground stations (USC, GREAT)
Observation period	3 years
Uncertainty of tensor-to-scalar ratio r	$\delta r < 1 \times 10^{-3}$
Multipole moment	$2 \leqq l \leqq 200$
Orbit	Second Sun–Earth Lagrangian point L2; Lissajous orbit
Scan	Precession angle 45° (10^{-2}–10^{-3} rpm); spin angle 50° (0.05–0.1 rpm)
Pointing knowledge	< 2.1 arcmin
Cooling system	Radiative cooling and mechanical refrigerators (Stirling and JT) without cryogens. Cool in space after launch. ADRs are used to cool the focal plane down to 100 mK
Focal-plane detector	Multichroic superconducting detector arrays with more than 4000 TES bolometers
Sensitivity	2 μK arcmin
Observing frequencies	15 bands between 34 and 448 GHz
Modulation	Satellite spin and half-wave plate modulation
Data transfer	9.6 GByte/day
Mass	2.6 ton
Electrical power	3.0 kW

Table 2 LiteBIRD telescope parameters

Telescope	Low freq.	Medium freq.	High freq.
Frequency	34–161 GHz	89–224 GHz	166–448 GHz
Telescope field of view	$20° \times 10°$	28° diameter	28° diameter
Aperture diameter	400 mm	300 mm	200 mm
Angular resolution	70–24 arcmin	38–28 arcmin	29–18 arcmin
Rotational HWP	46–83 rpm	39–70 rpm	61–110 rpm
Number of detectors	1248	2074	1354

instead, we have increased the number of detectors. With the international collaboration between Japan, the USA, Canada, and Europe, the satellite is planned to be launched with JAXA's H3 rocket in 2027FY (Fig. 1). Tables 1 and 2 summarize the updated basic parameters and current baseline design.

3 Current Design and Technical Progresses of LiteBIRD

3.1 Cooling Chain

With the design modification required, we have selected the following baseline combination for the cooling chain: (i) down to 5 K a sunshield and passive cooling with V-grooves [10], 15-K pulse tube coolers, and a 4-K J-T with 2ST precoolers; (ii) from 5 to 1.75 K a parallel three-stage ADR for providing continuous cooling at 1.75 K; and (iii) from 1.75 K to 100 mK a multistaged ADR with continuous cooling at 300 mK and 100 mK. Detailed schemes for this cooling chain are described in [11].

3.2 Telescopes and Polarization Modulator Units

The accurate, precise, and robust foreground cleaning requires 15 frequency bands covering a wide range of 34 to 448 GHz. This will be achieved with two kinds of telescopes (Table 2): a reflective one for the lower-frequency range (LFT) and refractive ones for medium- and high-frequency ranges (MHFT [12]). While the LFT uses crossed-Dragone reflective optics [13, 14] to minimize effects from multireflection among refractive surfaces, the MHFT uses lens optics with the advantage of compactness. For the LFT, the F#3.0 and the crossing angle of 90° have been selected, since this combination suppresses the straylight [9, 15] (Fig. 2), and aluminum is used as the mirror material [16]. All the telescopes are cooled down to 5 K for suppressing thermal noise.

Each telescope has a polarization modulator unit (PMU) [12, 17–19], which consists of a transmissive half-wave plate (HWP) system rotated with a superconductive magnetic bearing (SMB), as the first optical element, close to the aperture stop

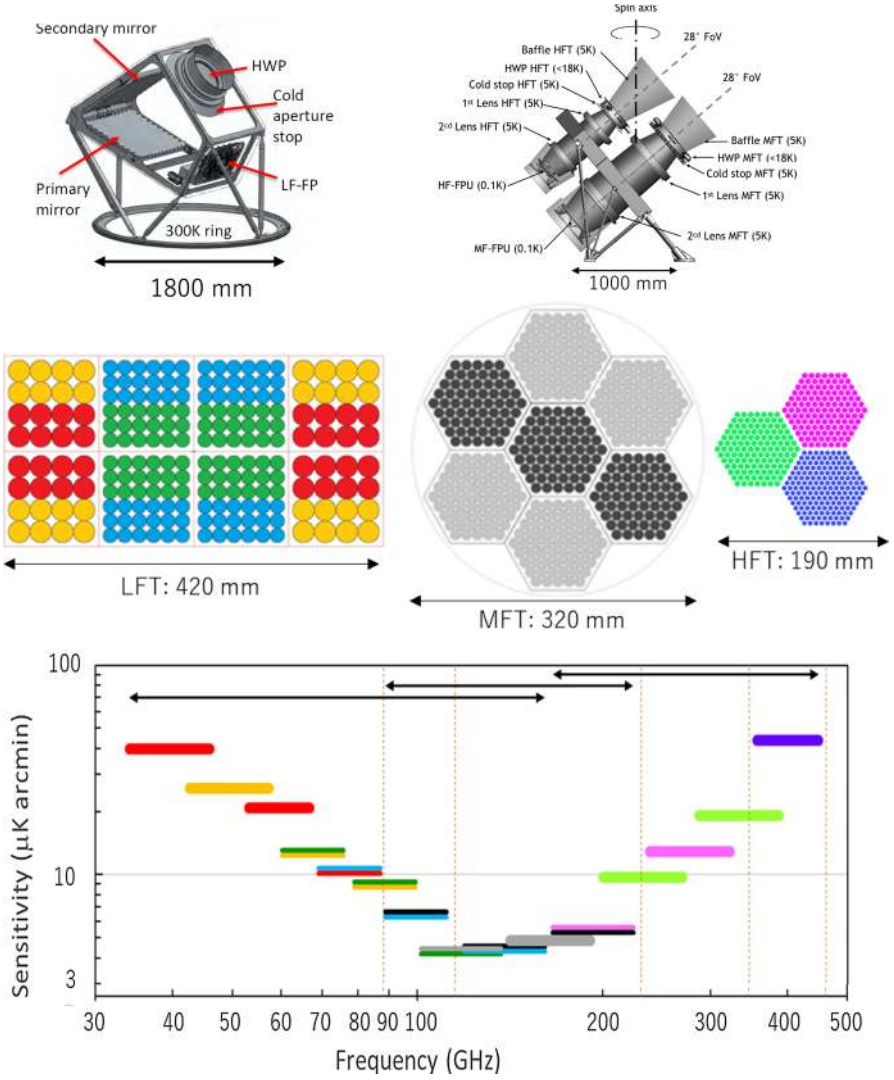

Fig. 2 *Top:* Designs of LFT (*left*) [9] and MHFT (*right*) [12]. *Middle:* Pixel distribution in LFT (*left*), MFT (*center*), and HFT (*right*) focal planes. Pixel diameters are: 23.6 mm for red (central frequencies of 40, 60, 78 GHz) and orange (50, 68, 89 GHz) pixels; 15.6 mm for green (68, 89, 119 GHz) and light blue (78, 100, 140 GHz) pixels in LFT; 11.6 mm for black (100, 140, 195 GHz) and gray (119, 166 GHz) pixels in MFT; 6.6 mm for pink (195, 280 GHz) and light green (235, 337 GHz) pixels; and 5.7 mm for blue (402 GHz) pixels in HFT. *Bottom:* Predicted LiteBIRD sensitivity. Colors correspond to those shown in the pixel distributions. Frequency ranges for LFT, MFT, and HFT are shown with black arrows. Frequencies of CO $J=1$–0, 2–1, 3–2, 4–3 and HCN $J=1$–0 lines are shown as thin vertical brown dashed lines. Total sensitivity is 2 μK arcmin. (Color figure online)

to distinguish the sky and instrumental polarization components and to reduce the instrumental 1/*f* noise. The SMB enables contactless operation of the HWP system, which minimizes heat generation, through magnetic levitation by using YBCO bulk

and permanent SmCo magnets. The LFT HWP system consists of multilayer stacked sapphire HWPs with optical axes shifted relative to each other to achieve high polarization efficiency over the wide frequency range [20], while the MHFT employs the metal-mesh HWPs [19]. At the top and bottom surfaces of the LFT HWP system, we adopt anti-reflection with sub-wavelength structure produced by laser machining. A cryogenic testbed is designed to study interactions, such as between space-optimized detectors and the PMU, consisting of a magnetically levitated and rotating HWP system [21].

3.3 Detectors and Readout

Transition-edge sensor (TES) bolometers are used to form multichroic pixels, based on maturity from successful ground-based and balloon experiments [22]. TES bolometers are coupled with a silicon lenslet and a sinuous antenna for individual broadband pixels for LFT and MFT, while silicon platelet-based corrugated horn and orthomode transducers are used for HFT [23, 24]. The noise equivalent power of TES bolometer is proportional to $\sqrt{(P_{\rm sat}\, T_{\rm b})}$, with the $T_{\rm c}/T_{\rm b}$ ratio being optimized. Here, $P_{\rm sat}$, $T_{\rm c}$, and $T_{\rm b}$ are the saturated power, transition temperature, and thermal bath temperature, respectively. The TES parameter optimization for LiteBIRD, toward low-saturation power detectors for the satellite environment, has been carried out, as well as a sensor impedance that readily couples to the frequency-domain multiplexer. The electro-thermal time constants are controlled by slowing down with the additional heat capacity. Details of these experimental results are described in [25]. Cosmic ray mitigation methods have been developed by reducing propagation with palladium structures to absorb phonons and with the removal of bulk silicon to block phonons [26]. Readout will be carried out through digital frequency multiplexing, with 68 bolometers connected to each SQUID array amplifier [27, 28]. The updated focal-plane designs and the expected sensitivities are shown in Fig. 2.

4 Foreground-Cleaning and Systematic Uncertainty Studies

The focal-plane designs have been determined through iterations with sensitivity calculations based on thermal studies [10], as well as with foreground-cleaning (by using methods described in [29–32]) and systematic uncertainty studies. The baseline foreground-cleaning results have been obtained based on an eight-dimensional parameterization of the foregrounds, including synchrotron power-law spectral index plus curvature and effective temperature of dust, plus power-law index of dust emissivity for Q and U Stokes parameters, each of which is allowed to vary across the sky. Systematic uncertainties have also been studied [33], including beam systematics [14], instrumental polarization and HWP harmonics, polarization efficiency, relative and absolute gain, pointing, polarization angle, time-correlated noise, cosmic ray glitches, bandpass mismatch [34], transfer function, nonlinearity, and non-uniformity in HWP, with realistic ground/in-flight calibration methods taken into account [e.g., 15, 35]. Through all these studies, it has been shown that the

updated focal-plane designs satisfy LiteBIRD's full success of the total uncertainty in the tensor-to-scalar ratio of less than 0.001, with its uncertainty budgets distributed comparably into a statistical part (including foreground residual and lensing B-mode), a systematic part, and a margin.

Acknowledgements This work was supported by World Premier International Research Center Initiative (WPI), MEXT, Japan, by JSPS Core-to-Core Program, A. Advanced Research Networks, and by JSPS KAKENHI Grant Numbers JP15H05891, JP17H01115, and JP17H01125. The Italian contribution to the LiteBIRD phase A is supported by the Italian Space Agency (ASI Grant No. 2016-24- H.1-2018) and the National Institute for Nuclear Physics (INFN). The French contribution to the LiteBIRD phase A is supported by the Centre National d'Etudes Spatiale (CNES), by the Centre National de la Recherche Scientifique (CNRS), and by the Commissariat à l'Energie Atomique (CEA). A Concurrent Design Facility study focused on the MHFT and Sub-Kelvin coolers has been led by the European Space Agency (ESA). The Canadian contribution to LiteBIRD is supported by the Canadian Space Agency. The US contribution is supported by NASA Grant no. 80NSSC18K0132.

Open Access This article is licensed under a Creative Commons Attribution 4.0 International License, which permits use, sharing, adaptation, distribution and reproduction in any medium or format, as long as you give appropriate credit to the original author(s) and the source, provide a link to the Creative Commons licence, and indicate if changes were made. The images or other third party material in this article are included in the article's Creative Commons licence, unless indicated otherwise in a credit line to the material. If material is not included in the article's Creative Commons licence and your intended use is not permitted by statutory regulation or exceeds the permitted use, you will need to obtain permission directly from the copyright holder. To view a copy of this licence, visit http://creativecommons.org/licenses/by/4.0/.

References

1. A.A. Starobinsky, Phys. Lett. **91B**, 99–102 (1980)
2. K. Sato, Mon. Notices. R. Astron. Soc. **195**, 467–479 (1981)
3. A.H. Guth, Phys. Rev. D **23**, 347–356 (1981)
4. U. Seljak, M. Zaldarriaga, Phys. Rev. Lett. **78**, 2054–2057 (1997)
5. M. Kamionkowski, A. Kosowsky, A. Stebbins, Phys. Rev. Lett. **78**, 2058–2061 (1997)
6. M. Hazumi et al., J. Low Temp. Phys. **194**, 443–452 (2019). https://doi.org/10.1007/s10909-019-02150-5
7. S. Takakura et al., Astrophys. J. **870**, 102 (2019). https://doi.org/10.3847/1538-4357/aaf381
8. A. Miniussi et al., J. Low Temp. Phys. **176**, 815–821 (2014). https://doi.org/10.1007/s10909-014-1104-x
9. Y. Sekimoto et al., SPIE Proc. **10698**, 106981Y (2018). https://doi.org/10.1117/12.2313432
10. T. Hasebe et al., SPIE Proc. **10698**, 1069864 (2018). https://doi.org/10.1117/12.2313034
11. J.-M. Duval, et al., J. Low Temp. Phys. **This Special Issue** (2020) (in press)
12. B. Mot, et al., J. Low Temp. Phys. **This Special Issue** (2020) (in press)
13. S. Kashima, M. Hazumi, H. Imada, N. Katayama, T. Matsumura, Y. Sekimoto, H. Sugai, Appl. Opt. **57**, 4171–4179 (2018). https://doi.org/10.1364/AO.57.004171
14. H. Imada et al., SPIE Proc. **10698**, 106984K (2018). https://doi.org/10.1117/12.2312185
15. H. Takakura et al., IEEE Trans. Terahertz Sci. Technol. **9**, 598 (2019). https://doi.org/10.1109/TTHZ.2019.2937497
16. H. Sugai et al., SPIE Proc. **10372**, 103720I (2017). https://doi.org/10.1117/12.2273765
17. Y. Sakurai et al., SPIE Proc. **10708**, 107080E (2018). https://doi.org/10.1117/12.2312391
18. F. Columbro, P. de Bernardis, S. Masi, Rev. Sci. Instrum. **89**, 125004 (2018). https://doi.org/10.1063/1.5035332
19. G. Pisano et al., SPIE Proc. **9153**, 915317 (2014). https://doi.org/10.1117/12.2056380
20. K. Komatsu et al., SPIE Proc. **10708**, 1070847 (2018). https://doi.org/10.1117/12.2312431

21. T. Ghigna, et al., J. Low Temp. Phys. **This Special Issue** (2020). https://doi.org/10.1007/s10909-020-02359-9
22. A. Suzuki, et al., J. Low Temp. Phys. **This Special Issue** (2020). https://doi.org/10.1007/s10909-019-02325-0
23. B. Westbrook, et al., J. Low Temp. Phys. **This Special Issue** (2020) (in press)
24. A. Suzuki et al., J. Low Temp. Phys. **193**, 1048–1056 (2018). https://doi.org/10.1007/s10909-018-1947-7
25. G. Jaehnig, et al., J. Low Temp. Phys. **This Special Issue** (2020) (in press)
26. Y. Minami, et al., J. Low Temp. Phys. **This Special Issue** (2020) (in press)
27. M. Tsujimoto et al., SPIE Proc. **10698**, 1069847 (2018). https://doi.org/10.1117/12.2311579
28. A. Lowitz, A. Bender, M.A. Dobbs, A. Gilbert, SPIE Proc. **10708**, 107081D (2018). https://doi.org/10.1117/12.2311984
29. J. Errard, R. Stompor, arXiv:1811.00479v1 (2018)
30. M. Remazeilles, C. Dickinson, H.K.K. Eriksen, I.K. Wehus, Mon. Notices. R. Astron. Soc. **458**, 2032–2050 (2016). https://doi.org/10.1093/mnras/stw441
31. H.K. Eriksen, J.B. Jewell, C. Dickinson, A.J. Banday, K.M. Górski, C.R. Lawrence, Astrophys. J. **676**, 10–32 (2008). https://doi.org/10.1086/525277
32. K. Ichiki, H. Kanai, N. Katayama, E. Komatsu, Prog. Theor. Exp. Phys. **2019**, 033E01 (2019). https://doi.org/10.1093/ptep/ptz009
33. H. Ishino et al., SPIE Proc. **9904**, 99040X (2016). https://doi.org/10.1117/12.2231995
34. D.-T. Hoang et al., J. Cosmol. Astropart. Phys. **2017**, 015 (2017). https://doi.org/10.1088/1475-7516/2017/12/015
35. Y. Minami, H. Ochi, K. Ichiki, N. Katayama, E. Komatsu, T. Matsumura arXiv: 1904.12440v1 (2019)

Publisher's Note Springer Nature remains neutral with regard to jurisdictional claims in published maps and institutional affiliations.

Affiliations

H. Sugai[40] · P. A. R. Ade[62] · Y. Akiba[41,52] · D. Alonso[67] · K. Arnold[75] · J. Aumont[11] · J. Austermann[72] · C. Baccigalupi[19,25,27] · A. J. Banday[11] · R. Banerji[57] · R. B. Barreiro[59] · S. Basak[16,27] · J. Beall[72] · S. Beckman[74] · M. Bersanelli[22,30] · J. Borrill[70,74] · F. Boulanger[9] · M. L. Brown[66] · M. Bucher[5] · A. Buzzelli[29] · E. Calabrese[62] · F. J. Casas[59] · A. Challinor[63,65] · V. Chan[4] · Y. Chinone[40,74] · J.-F. Cliche[1] · F. Columbro[24,26] · A. Cukierman[74] · D. Curtis[74] · P. Danto[7] · P. de Bernardis[24,26] · T. de Haan[70] · M. De Petris[24,26] · C. Dickinson[66] · M. Dobbs[1] · T. Dotani[37] · L. Duband[6] · A. Ducout[40] · S. Duff[72] · A. Duivenvoorden[61] · J.-M. Duval[6] · K. Ebisawa[37] · T. Elleflot[75] · H. Enokida[35] · H. K. Eriksen[57] · J. Errard[5] · T. Essinger-Hileman[71] · F. Finelli[20] · R. Flauger[75] · C. Franceschet[22,30] · U. Fuskeland[57] · K. Ganga[5] · J.-R. Gao[56] · R. Génova-Santos[58,60] · T. Ghigna[40,67] · A. Gomez[7] · M. L. Gradziel[17] · J. Grain[9] · F. Grupp[14,15] · A. Gruppuso[20] · J. E. Gudmundsson[61] · N. W. Halverson[76] · P. Hargrave[62] · T. Hasebe[37] · M. Hasegawa[41,52] · M. Hattori[53] · M. Hazumi[37,40,41,52] · S. Henrot-Versille[12] · D. Herranz[59] · C. Hill[70,74] · G. Hilton[72] · Y. Hirota[35] · E. Hivon[8] · R. Hlozek[4] · D.-T. Hoang[68,77] · J. Hubmayr[72] · K. Ichiki[45] · T. Iida[40] · H. Imada[12] · K. Ishimura[54] · H. Ishino[41,48] · G. C. Jaehnig[76] · M. Jones[67] · T. Kaga[37] · S. Kashima[46] · Y. Kataoka[48] ·

N. Katayama[40] · T. Kawasaki[42] · R. Keskitalo[70] · A. Kibayashi[48] · T. Kikuchi[32] · K. Kimura[49] · T. Kisner[70] · Y. Kobayashi[38] · N. Kogiso[49] · A. Kogut[71] · K. Kohri[41] · E. Komatsu[13] · K. Komatsu[48] · K. Konishi[36] · N. Krachmalnicoff[19,25,27] · C. L. Kuo[69,73] · N. Kurinsky[69,73] · A. Kushino[44] · M. Kuwata-Gonokami[34] · L. Lamagna[24,26] · M. Lattanzi[21] · A. T. Lee[70,74] · E. Linder[70,74] · B. Maffei[9] · D. Maino[22,30] · M. Maki[41] · A. Mangilli[11] · E. Martínez-González[59] · S. Masi[24,26] · R. Mathon[11] · T. Matsumura[40] · A. Mennella[22,30] · M. Migliaccio[24,29] · Y. Minami[41] · K. Mistuda[37] · D. Molinari[28] · L. Montier[11] · G. Morgante[20] · B. Mot[11] · Y. Murata[37] · J. A. Murphy[17] · M. Nagai[46] · R. Nagata[41] · S. Nakamura[55] · T. Namikawa[65] · P. Natoli[21,28] · S. Nerval[4] · T. Nishibori[39] · H. Nishino[50] · Y. Nomura[51] · F. Noviello[62] · C. O'Sullivan[17] · H. Ochi[55] · H. Ogawa[49] · H. Ogawa[37] · H. Ohsaki[35] · I. Ohta[43] · N. Okada[37] · N. Okada[49] · L. Pagano[21,28] · A. Paiella[24,26] · D. Paoletti[20] · G. Patanchon[5] · F. Piacentini[24,26] · G. Pisano[62] · G. Polenta[18] · D. Poletti[19,25,27] · T. Prouvé[6] · G. Puglisi[73] · D. Rambaud[11] · C. Raum[74] · S. Realini[22,30] · M. Remazeilles[66] · G. Roudil[11] · J. A. Rubiño-Martín[58,60] · M. Russell[75] · H. Sakurai[34] · Y. Sakurai[40] · M. Sandri[20] · G. Savini[64] · D. Scott[3] · Y. Sekimoto[37,41,52] · B. D. Sherwin[63,65] · K. Shinozaki[39] · M. Shiraishi[47] · P. Shirron[71] · G. Signorelli[23] · G. Smecher[2] · P. Spizzi[7] · S. L. Stever[40] · R. Stompor[5] · S. Sugiyama[51] · A. Suzuki[70] · J. Suzuki[41] · E. Switzer[71] · R. Takaku[34] · H. Takakura[33] · S. Takakura[40] · Y. Takeda[37] · A. Taylor[67] · E. Taylor[74] · Y. Terao[35] · K. L. Thompson[69,73] · B. Thorne[67] · M. Tomasi[22,30] · H. Tomida[37] · N. Trappe[17] · M. Tristram[12] · M. Tsuji[47] · M. Tsujimoto[37] · C. Tucker[62] · J. Ullom[72] · S. Uozumi[48] · S. Utsunomiya[40] · J. Van Lanen[72] · G. Vermeulen[10] · P. Vielva[59] · F. Villa[20] · M. Vissers[72] · N. Vittorio[29] · F. Voisin[5] · I. Walker[62] · N. Watanabe[42] · I. Wehus[57] · J. Weller[14,15] · B. Westbrook[74] · B. Winter[64] · E. Wollack[71] · R. Yamamoto[32] · N. Y. Yamasaki[37] · M. Yanagisawa[48] · T. Yoshida[37] · J. Yumoto[34] · M. Zannoni[22,31] · A. Zonca[75]

✉ H. Sugai
hajime.sugai@ipmu.jp

[1] McGill University, Montreal, Canada

[2] Three-Speed Logic, Inc., Victoria, Canada

[3] University of British Columbia, Vancouver, Canada

[4] University of Toronto, Toronto, Canada

[5] APC, CNRS, University Paris Diderot, Paris, France

[6] Univ. Grenoble Alpes, CEA, Grenoble, France

[7] CNES, Paris, France

[8] IAP, Sorbonne University, Paris, France

[9] IAS, Université Paris-Saclay, CNRS, Orsay, France

[10] Institut Néel, Grenoble, France

[11] IRAP, University de Toulouse, CNRS, CNES, UPS, Toulouse, France

[12] LAL, CNRS/IN2P3, University Paris-Saclay, Orsay, France

[13] MPA, Garching, Germany

[14] MPE, Garching, Germany
[15] University Observatory Munich, Ludwig-Maximimilians University Munich, Munich, Germany
[16] IISER-TVM, Thiruvananthapuram, India
[17] National University of Ireland Maynooth, Maynooth, Ireland
[18] ASI, Rome, Italy
[19] IFPU, Grignano, Italy
[20] INAF – OAS Bologna, Bologna, Italy
[21] INFN Ferrara, Ferrara, Italy
[22] INFN Milano, Milan, Italy
[23] INFN Pisa, Pisa, Italy
[24] INFN Roma, Rome, Italy
[25] INFN Trieste, Trieste, Italy
[26] Sapienza University of Rome, Rome, Italy
[27] SISSA, Trieste, Italy
[28] University di Ferrara, Ferrara, Italy
[29] University di Roma Tor Vergata, Rome, Italy
[30] University of Milano, Milan, Italy
[31] University of Milano Bicocca, Milan, Italy
[32] AIST, Tsukuba, Japan
[33] Department of Astronomy, University of Tokyo, Tokyo, Japan
[34] Department of Physics, University of Tokyo, Tokyo, Japan
[35] GSFS, University of Tokyo, Kashiwa, Japan
[36] IPST, University of Tokyo, Tokyo, Japan
[37] ISAS, JAXA, Sagamihara, Japan
[38] ISSP, University of Tokyo, Kashiwa, Japan
[39] JAXA, Tsukuba, Japan
[40] Kavli IPMU (WPI), University of Tokyo, Kashiwa, Japan
[41] KEK, Tsukuba, Japan
[42] Kitasato University, Sagamihara, Japan
[43] Konan University, Kobe, Japan
[44] Kurume University, Kurume, Japan
[45] Nagoya University, Nagoya, Japan
[46] NAOJ, Mitaka, Japan
[47] National Institute of Technology, Kagawa College, Takamatsu, Japan
[48] Okayama University, Okayama, Japan
[49] Osaka Prefecture University, Sakai, Japan
[50] RESCEU, University of Tokyo, Tokyo, Japan
[51] Saitama University, Saitama, Japan

[52] SOKENDAI, Hayama, Japan
[53] Tohoku University, Sendai, Japan
[54] Waseda University, Tokyo, Japan
[55] Yokohama National University, Yokohama, Japan
[56] SRON, Utrecht, The Netherlands
[57] University of Oslo, Oslo, Norway
[58] IAC, Santa Cruz de Tenerife, Spain
[59] IFCA, CSIC-Univ de Cantabria, Santander, Spain
[60] University de La Laguna, Santa Cruz de Tenerife, Spain
[61] Stockholm University, Stockholm, Sweden
[62] Cardiff University, Cardiff, UK
[63] KICC, Cambridge, UK
[64] University College London, London, UK
[65] University of Cambridge, Cambridge, UK
[66] University of Manchester, Manchester, UK
[67] University of Oxford, Oxford, UK
[68] Cornell University, Ithaca, USA
[69] KIPAC, Menlo Park, USA
[70] LBNL, Berkeley, USA
[71] NASA Goddard, Greenbelt, USA
[72] NIST, Boulder, USA
[73] Stanford University, Stanford, USA
[74] University of California, Berkeley, USA
[75] University of California, San Diego, USA
[76] University of Colorado, Boulder, USA
[77] USTH, Hanoi, Vietnam